Post-flooding disturbance recovery promotes carbon capture in riparian zones

Yihong Zhu[1, 4#], Ruihua Liu[2,4#], Huai Zhang[2], Shaoda Liu[3], Zhengfeng Zhang[2], Feihai Yu[5], Timothy G. Gregoire[4]

[1]Department of Environmental Science, Policy and Management, University of California, Berkeley, 94704, USA
[2]School of Earth and Planetary, University of Chinese Academy of Sciences, Beijing, 100049, China
[3]State Key Laboratory for Water Environment Simulation, School of Environment, Beijing Normal University, Beijing, 100875, China
[4]Yale School of the Environment, Yale University, New Haven, 06511, USA
[5]Institute of Wetland Ecology & Clone Ecology; Zhejiang Provincial Key Laboratory of Plant Evolutionary Ecology and Conservation, Taizhou University, Thaizhou, 318000, China
[#]Yihong Zhu and Ruihua Liu contributed equally to this paper.

Correspondence to: Shaoda Liu (liushaoda@bnu.edu.cn); Huai Zhang (hzhang@ucas.ac.cn)

Abstract. Vegetation, water, and carbon dioxide have complex interactions on carbon mitigation in vegetation-water ecosystems. As one of the major global change drivers of carbon sequestration, flooding disturbance is a fundamental but poorly discussed topic to date. The aquatic and associated riparian systems are highly dynamic vegetation-water carbon capture systems driven by fluvial processes such as flooding. However, their global carbon offset potential is largely unknown. This study examines daily CO_2 perturbations in the river and associated riparian areas with two-year in-situ observations along the Lijiang River. We find that, though the submerged riparian area behaved as a carbon source during the flooding season (CO_2 flux: 2.790 $g \cdot m^{-2} \, d^{-1}$), the riparian area and the fluvial area as a whole transformed from a carbon source in pre-flooding season (1.833 $g \cdot m^{-2} \, d^{-1}$) to a carbon sink after recovery in post-flooding season (-0.592 $g \cdot m^{-2} \, d^{-1}$). The fluvial area sequestered carbon (-0.619 $g \cdot m^{-2} \, d^{-1}$) in post-flooding season instead of releasing carbon as in pre-flooding season (2.485 $g \cdot m^{-2} \, d^{-1}$). Also, the carbon sequestration capacity of the riparian area was enhanced in post-flooding season (pre-flooding season: -0.156 $g \cdot m^{-2} \, d^{-1}$, post-flooding season: -0.500 $g \cdot m^{-2} \, d^{-1}$). We suggest post-disturbance recovery of riparian vegetation played a vital role in this transformation, due to its stronger carbon uptake capacity after recovery from the flooding disturbances. ~~Consequently, a quantitative global riparian carbon offset model is proposed. Based on the intensity of flooding submergence and post-flooding vegetation coverage, -0.11Gt·year⁻¹ CO₂ is captured following flooding, and 0.53 Gt·year⁻¹ more CO₂ is captured due to flooding, which is equivalent to 9.1 % of the global forest carbon sequestration.~~ The findings shed light on the quantitative modelling of the riparian carbon cycle under flooding disturbance and underlined the importance of the proper restoration of riparian systems to achieve global carbon offset.

1 Introduction

Climate change issues stemming from anthropogenic carbon emissions have strengthened dramatically, immensely threatening
35   ecosystem stability and biodiversity (Li et al., 2022; Wang et al., 2020). The increasing atmospheric CO_2 originating from fossil fuel combustion and industrial activities can be regulated by plant metabolism (photosynthesis and respiration) and soil microbial activities (Zheng et al., 1998). In general, the net carbon emission strongly depends on the balance between the production and consumption processes in the vulnerable natural ecosystem (Pugh et al., 2019).

40   Aquatic and associated riparian systems are highly dynamic systems driven by fluvial processes (e.g.: flooding and deposition of alluvial soil) (Naiman and Decamps, 1997; Steiger et al., 2005). Riparian zones are generally defined as a complex terrestrial assemblage of plants and other organisms adjacent to an aquatic environment. For instance, the interface between aquatic and terrestrial environments in coniferous forests forms a narrow riparian zone (Gregory et al., 1991). Riparian zones are of great importance in carbon cycling, which is associated with the production and consumption of CO_2 and methane (CH_4) (Zhang et
45   al., 2016; Allen et al., 2007; Liu et al., 2021).

Riparian zone is often considered as sinks for CO_2 through photosynthetic assimilation of CO_2 in atmosphere, but disturbance may turn it from carbon sink to carbon source. Seasonal periodic flooding is one of the most common environmental disturbances in riparian zones. Floods can be natural, but human activity such as the construction of dams increasingly
50   causes controlled floods (Darrel Jenerette and Lal, 2005; Dynesius and Nilsson, 1994). Flooding disturbance strongly influences the biotic characteristics of riparian assemblages (Anderson et al., 2020) as well as the carbon cycle. Flooding could increase soil respiration and enzymatic degradation rate (Wilson et al., 2011). It was found that the rate of CO_2 emission in riparian wetlands is higher than that in neighbouring hillslope grasslands (Anderson et al., 2020). Liu et al. (2021) demonstrated that high plant and soil respiration in riparian wetlands lead to large amounts of CO_2 emission in wet season (335-2790 mg·m^{-2}h^{-1})
55   ^{2}h^{-1}) than in dry season (72 - 387 mg·m^{-2}h^{-1}) (Liu et al., 2021). Also, the short-term anaerobic conditions caused by flooding may increase the production of methane because of the strengthened methanogenesis in riparian soils (Hassanzadeh et al., 2019; Hondula et al., 2021; Morse et al., 2012; Le Mer and Roger, 2001; Thorp et al., 2006).

The influence of flooding disturbance would also depend on the flooding characteristics and the properties of riparian soils.
60   Hirota et al. (2007) found that temporal variations of the greenhouse gases fluxes were strongly manipulated by water-level fluctuations in the sandy shore and by soil temperature in the salt marsh (Hirota et al., 2007). The duration of flooding was also considered an important factor for riparian carbon dynamics and microbial community structure (Wilson et al., 2011). The spatial heterogeneity of soil properties would also affect the composition and diversity of bacterial communities in riparian zones and thus may influence the riparian carbon cycle under flooding disturbance (Wang et al., 2019b; Wilson et al., 2011).

65

Strong seasonality for different greenhouse gas emissions has been detected in previous studies (Gaughan and Waylen, 2012; Allen et al., 2007). With flooding disturbance, riparian vegetation plays an indispensable role in sequestering carbon (Maraseni and Mitchell, 2016) and the variations in riparian vegetation communities are expected to define the ecological role of riparian zones in carbon cycle. During flooding season, flooding submergence may impede gas diffusion and decrease light intensity,

70 leading to high mortality and limited growth of plant species (Colmer et al., 2009). This raises the possibility of elevated carbon (including methane and carbon dioxide) emissions and reduced carbon sequestration from riparian zones, shifting the role of riparian zones from a carbon sink to a carbon source. Conversely, as riparian species adapt to flooding submergence and recover from flooding, riparian zones may gradually return to the initial status or even promote CO_2 capture. Previous studies found that riparian vegetation may increase their leaf gas exchange in response to submergence stress so as to cope with oxygen

75 limitation (Huang et al., 2017; Mommer et al., 2006; Liu et al., 2020). Besides, inundation depth increased reed density, height, leaf area index and biomass, and thus decreased the global warming potential during the growing season (Zhao et al., 2020). Therefore, riparian zone may oscillate between carbon source and sink depending on flooding. It raises the open question of whether riparian zones quantitatively promote or hinder carbon capture overall.

80 Flooding is one of the most common forms of environmental disturbance in riparian zones, which strongly influences the biotic characteristics of riparian assemblages (Anderson et al., 2020). Floods can be natural, but human activity such as the construction of dams increasingly causes controlled floods (Darrel Jenerette and Lal, 2005; Dynesius and Nilsson, 1994). Variations in riparian vegetation communities are expected to define the ecological role of riparian zones in carbon cycle. Flooding submergence may impede gas diffusion and decrease light intensity, leading to high mortality and limited plant

85 individuals (Colmer et al., 2009). This raises the possibility that riparian zones may promote carbon emission, shifting the role of riparian zones from carbon sink to the carbon source. It is supported by the fact that the rate of CO_2 emission in riparian wetlands is higher than that in neighbouring hillslope grasslands (Anderson et al., 2020).

Disturbances in vulnerable ecosystems like riparian zones may change the system from carbon sinks to carbon sources

90 (Running, 2008). Disturbances have the potential to both augment and offset the carbon loading of the atmosphere attributed to anthropogenic carbon emissions (Sierra et al., 2017). Carbon capture can be promoted by lengthening the growing season and expanding the niches from which water can be drawn (Mahanta et al., 2020). On the contrary, carbon emission can be promoted by pervasive growth lifespan trade-offs as it happens in forests (Brienen et al., 2020; Gatti et al., 2021). Since three-quarters of disturbances are directly human-induced (Venter et al., 2016), a better understanding of the role of disturbance on

95 vegetation in the carbon cycle is highly relevant to reducing carbon emission (Pugh et al., 2019).

The indispensable role of riparian vegetations in sequestering carbon is increasingly underlined in the context of global climate change (Maraseni and Mitchell, 2016). Riparian vegetations are often considered as sinks for CO_2 through the pathway of photosynthetic assimilation of CO_2 and carbon sequestration in soil under anaerobic conditions. They are also a potential CH_4

100 source in the natural environment (Hassanzadeh et al., 2019; Hondula et al., 2021; Morse et al., 2012). Liu et al. (2021) demonstrated that high plant and soil respiration in riparian wetlands may lead to larger amounts of CO_2 emission than CH_4 detected in the wet season (wet season: 335-2790 mg·m^{-2}h^{-1}; dry season: 72-387 mg·m^{-2}h^{-1}) (Liu et al., 2021). Conversely, as riparian species recover after flooding, riparian zones can promote CO_2 capture. Considering different types of water fluctuations, Hirota et al. (2007) compared three greenhouse gas fluxes in the sandy shore and salt marsh of a coastal lagoon

105 in Japan. They find that temporal variations of the fluxes are strongly manipulated by water-level fluctuations in the salt marsh's sandy shore and soil temperature (Hirota et al., 2007). Therefore, riparian zones oscillate between a carbon source and sink depending on flooding. It raises the open question of whether riparian zones quantitatively promote or hinder carbon capture overall.

110 Riparian zone is believed to have considerable potential to contribute to biodiversity, carbon sequestration, and several other ecosystem services. As a traditional practice, riparian vegetation has been cleared for crop and pasture production in numerous places worldwide, leading to increases in greenhouse gas emissions (Maraseni and Cockfield, 2011). It is noteworthy that proper and efficient restoration of the riparian zones is fundamental for the proper functioning of riparian ecosystem services. Thus, it has been listed as a priority in the IPCC community (Bullock et al., 2011). However, the current research on the

115 riparian carbon sequestration under flooding disturbance remains poorly constrained. There has been some modelling work about the riparian carbon stock, but fewer on the carbon flux. For instance, Dybala et al., (2019) modelled the change in carbon stock as a function of vegetation age, considering effects of climate and whether or not the riparian forest had been actively planted (Dybala et al., 2019). One limitation for models like Riparian Ecosystem Management Model (REMM) or other riparian models is that they require a large amount of site specific parameters, many of which are often modeled using other

120 models as inputs (Vidon et al., 2019). In addition to climatic factors, factors such as floodplain width, flow regime, frequency of inundation, and the presence of dams, diversions, and levees also need to be considered when modelling the riparian carbon flux with the disturbance of flooding (Sutfin et al., 2016).

In order to figure out how floods affect the balance between carbon emission and sequestration in riparian areas, we quantified

125 the vertical CO_2 fluxes at the soil-air interface and water-air interface during the flooding season and non-flooding seasons (pre-flooding season and post-flooding season) based on two-year in-situ measurements along the Lijiang River. Considering an overall small contribution of CH_4 to the carbon balance of riparian zones (Liu et al., 2021; Vidon et al., 2019), only CO_2 fluxes were measured in analysis. We establish that a riparian system promotes carbon capture despite enhanced carbon releases during flooding periods and its capacity is directly related to the resilience and post-disturbance recovery of riparian

130 vegetation. We suggest that promoting the recovery of riparian systems and establishing high flooding-tolerant vegetation coverage is key to promoting carbon capture in the context of increasing flood risks under climate change. Therefore, this work reveals how water disturbance affects the balance between carbon emission and carbon sequestration in water vegetation diverse areas. It quantitatively estimates the effect of flooding disturbance on riparian carbon dynamics. Eventually, we build

4

~~a quantitative riparian carbon offset model based on the disturbance intensity and post-vegetation coverage to evaluate the~~
135 ~~global carbon change due to flooding.~~

2 Methods

2.1 In-situ observation setup

Our study site is in the downstream of the 164 kilometres lo ng Lijiang River in the Pearl River Basin in northwestern Guangxi
140 Zhuang Autonomous Province, Southwest China (25° 06′ N, 110° 25′; Fig. A1). Lijiang River has a typical karst landscape, with widely exposed carbonate rocks (Wang et al., 2019b). The river from Guilin to Yangshuo is the most typical karst development area. The river channel is composed of sand and pebbles, and the soil type is red loam with high sand content (Wang et al., 2019b). This area experiences a monsoon-based humidity subtropical climate, where the mean annual rainfall is 1900 mm, and the annual temperature ranges from 7.9 °C to 28.0 °C. In the dry season (normally September to March next
145 year), the minimum daily average flow discharge is often below 20 m³/s. Therefore, drought stress profoundly influences the early-stage development of riparian species. By contrast, in the flooding season (April to August), discharges over 1000 m³/s are common during flood events, inner islands are completely submerged, and some riparian species cease to grow or are destroyed. The soils of the Lijiang River riparian zone are sand-based, with sand contents ranging from 74.99% to 88.44%; silt and clay contents are lower, accounting for approximately 10% (Wang et al., 2019b; Lu and Wang, 2015). With the
150 decrease of inundation frequency, the sand content is found to decrease while the clay and silt content increased gradually (Wang et al., 2019b). Soil pH is around 6.99 to 7.71, and soil total nitrogen is around 0.93 to 1.40 (g·kg^{-1}) (Wang et al., 2019b). Different vegetation zones can further influence the chemical properties of soils (Lu and Wang, 2015).

2.2 Experiment design

2.2.1 Gas collection

155 Four transects were established on one island downstream of the Lijiang River (Fig. A1). The distance between each transect was approximately 3 m. Four subplots spaced 5-8 m apart were deployed in each transect, perpendicular to the waterlines and extended from the edge of the water body to the upper area. Site selection and chamber placement minimized differences in the microclimate among chamber stations. CO_2 in four 50 x 50 cm subplots along each transect were sampled by static chamber techniques. Four static chambers were used at each site (Fig. A1). Chambers were positioned in the same location for the
160 monitoring phase. On the river, floating static chambers were used (Sun et al., 2012) and were set up on shallow water and deep water. The floating static chamber was a cylindrical chamber (of radius 50cm and height 65cm) with a floating ring (about 20cm) around the bottom of the chamber to keep it floating on the water, and was thus sealed by the water. On the land during non-flooding seasons, the terrestrial static chambers (length 50 cm, width 50 cm, and height 50 cm) were used and were set up

on riparian areas with vegetation and without vegetation. The terrestrial static chamber was put on a stainless-steel underside base (length 50 cm, width 50 cm and height 15 cm) instead of setting directly on the ground. The underside base increased the chamber's size and prevented damage to the vegetation inside (Sun et al., 2013). There was a groove on the top of the underside base, and the upper portion of chamber was designed to be put into this groove. By adding water to the groove, the whole setting was sealed (Sun et al., 2012, 2013). The floating static chamber and the terrestrial static chamber both were covered by foam and reflective aluminium, which can easily reflect the heat from sunlight and thus prevent rapid temperature changes or temperature becoming too high in the chamber (Søvik and Kløve, 2007). Also, the chambers contained two exhaust fans, a thermometer and a tube inside. A syringe was used to collect gas samples from the tube at intervals of 0, 10, 20 and 30 minutes. For 24-hour monitoring, samples were taken every 4 hours (a total 6 times per day starting at 10:00 and finishing at 06:00 the next day) in one day in April, August, and October (covering pre-flooding season, flooding season, and post-flooding season) in 2014 (both riparian area and river) and 2016 (river). In other words, diel data was taken at the 0, 10min 20min and 30min of 10:00, 14:00, 18:00, 22:00, 2:00 and 6:00.

2.2.2 Measurement of gas concentration and hydro-environment condition

Gas samples were collected by a syringe from the tube of chamber and were instantly transferred to airtight glass bottles (20ml, Agilent5190-2286). All samples were analysed within three days. The CO_2 concentration was measured using gas chromatography (Agilent7890A) equipped with an electron capture detector (ECD) and a flame ionization detector (FID) (Agilent Technologies, 2010). The measurements were conducted by Pony Testing International Group Co. Ltd (300887:CH). Standard CO_2 gases (with concentration of 0 and 10000 pm, respectively) were used for method calibration. The calculation formula of CO_2 flux is

$$F = \frac{M}{V_0}\frac{P}{P_0}\frac{T_0}{T}H\frac{dc}{dt} \tag{1}$$

where F represents the gas flux ($\mu g \cdot m^{-2}\,h^{-1}$), M is the molar mass, V_0 represents the normal state of molar volume (22.4 L/mol), P_0 and T_0 are the pressure and temperature of the standard conditions (1013.25 hPa, 273.15 K) for gases, and d_c/d_t is the slope of the regression curve as gas concentration variable with time, respectively. The height of the chamber (H, cm), in-situ air pressure (P, hPa), and air temperature (T, K) were recorded during the sampling as well. The all-day CO_2 flux was calculated by integrating the diel CO_2 flux of different measuring times. The environmental information, including total organic carbon (TOC) and total inorganic carbon (TIC) downstream (Yangshuo Gauge) of the Lijiang River, was also recorded. Meanwhile, the water level was recorded hourly during the experiment period.

2.2.3 Vegetation inventory and flooding tolerant experiment

Vegetation inventory was conducted by three 15 m x 5 m transects along with this field site. Coverage, number of ramets, and height are measured. After the field inventory, about 300 seeds of *C. aciculatus*, which was the dominant riparian species after flooding, were sown in planting trays filled with peat (Pindstrup Seeding; Pindstrup Mosebrug A/S, Pindstrup, Denmark).

6

Seeds were bought from Forest Science Co, Ltd. of Beijing Forestry University. Eight grass plants with one single ramet were transplanted in the experimental pots. In total, 178 ramets with similar sizes of each species were selected for the experiment, of which 18 were randomly used to obtain their initial length and dry mass, and the remaining 80 ramets were used for the experiments. The initial ramet length of *C. aciculatus* was 9.56 ± 0.18 cm, and the dry mass was 38.56 ± 5.36 mg. The experiment lasted three months, from August 01 to November 01. The mean temperature and relative humidity were 26.21 ± 0.33 °C and 59.02 ± 1.46%, respectively. Sufficient tap water was added to each container to maintain the plant submerged in the water. At harvest, new ramets produced by each initial one were interconnected by aboveground stolon, so we could harvest and measure the growth attributes of plants in each treatment separately. We counted the number of ramets and weighed each plant's dry leaf, rhizome, and biomass in each container. All plant parts were oven-dried at 70°C for 72 h before weighing. The collection of materials complied with relevant institutional, national, and international guidelines and legislation.

2.2.4 Annual riparian and river CO_2 emission calculation

We are interested in whether or under what conditions the riparian area and the fluvial area as a whole can achieve carbon neutralization (which means the net carbon emission is zero) at the annual level with flooding disturbance. We take flooding disturbance into account by dividing the whole year into pre-flooding season, flooding season, and post-flooding season. We assume that flooding events happen at an annual timescale and consider the time that flooding would happen as flooding season. The occurrence of extreme weather like rainstorms or frost is not considered here. The riparian area refers to area that would be submerged during flooding. The field investigation showed that the riparian area in the non-flooding seasons (pre-flooding season and post-flooding season) was about 25% of the river width in the flooding season, and the vegetation coverage is about 60%. Thus, the annual riparian CO_2 emission is calculated as the sum of emissions in pre-flooding season, flooding season and post-flooding season, by the following equation:

$$C_{annual} = \sum C_{i,j} = \sum W_{i,j} * D_j * a_{i,j} \qquad (2)$$

Where C_{annual} is the annual expected carbon emission (C_{annual} =0 means the whole region reaches carbon neutralization at the annual level), $C_{i,j}$ is the annual CO_2 emission of river or riparian area in different seasons (i=1, 2 refer to river and riparian area respectively, j=1, 2, 3 refer to pre-flooding season, flooding season, and post-flooding season respectively), $W_{i,j}$ is the width of river or riparian area in different seasons, D_j is the days of corresponding season, and $a_{i,j}$ is the all-day CO_2 flux of river or riparian area in different seasons. Specially, during flooding season, the width of riparian area ($W_{1,2}$) is 0 meter because all the riparian area is submerged. The all-day CO_2 flux of riparian area in pre- ($a_{2,1}$) or post-flooding season ($a_{2,3}$) is calculated by the following equation:

$$a = a_{veg} * p + a_{soil} * (1 - p) \qquad (3)$$

Where a_{veg} is the all-day CO_2 flux of vegetation area, a_{soil} is the CO_2 flux of bare soil area, and p is the vegetation coverage.

2.2.5 Data analysis

For <u>riparian areas</u>, two-way repeated-measurement ANOVA were employed to examine the effects of vegetation (bare soil vs. land with vegetation; between-subject factor) and time (measuring times in one day, within-subject factor) on the CO_2 flux in two sampling stages (April: pre-flooding and October: post-flooding). For aquatic habitats <u>(fluvial area)</u>, two-way repeated-measures ANOVAs were used to examine the effects of sampling position (with vegetation vs. without vegetation or under water surface; between-subject factor) and time (measuring times in one day; within-subject factor) on CO_2 flux in sampling stages (April: pre-flooding, August: during flooding, and October: post-flooding). The p-values were calculated with the null hypothesis that the CO_2 flux of <u>riparian areas</u> or aquatic habits is not influenced by the factors mentioned. Before analyses, homogeneity of variance and normality are also examined. All data analyses were performed by the SPSS statistical software package (https://www.ibm.com/products/spss-statistics, version 22.0, Chicago, IL, USA). The effects were considered significant if p-value < 0.05.

2.3 Model scenario prediction method

2.3.1 Riparian carbon offset model

The carbon cycle considered in this model consists of the carbon flux of the terrestrial riparian zone (with bare soil and with vegetation) and the carbon flux of the river. Flooding events influence it in summer. We assume that flooding events happen at an annual timescale and consider the time that flooding would happen as flooding season. The area of the terrestrial riparian zone in this model refers to the area submerged during flooding. This model assumes that the terrestrial riparian zone in the dry season is 25% of the river width in the flooding season. We also assume the whole river to be a homogenously mixed reactor, so do not vary river morphometry. We do not consider the water temperature and the occurrence of extreme weather like rainstorms or frost.

$$C = \int_{p=0}^{1} D_\theta(p) \, dp$$

D is an impact or disturbance model, potentially consisting of both direct and indirect, tangible, and intangible components associated with flooding, along with certain event characteristics such as flood levels, extents, and durations, with an annual probability of non-exceedance p [1/T]. Finally, p represents a vegetation coverage of fixed-in-time factors, determining the vulnerability. Such factors eventually determine the shape of D. In brief, D_θ combines the exposure and vulnerability within an area into a disturbance function. The consequence D_θ of the event with vegetation coverage p can be expressed in a plethora of indicators, reflecting for disequilibrium of carbon neutralization. The associated vulnerability determining factors, θ, may differ depending on the type of consequence used to estimate them. The parameters used in this study can evaluate the carbon offset for rivers with similar biogeochemical characteristics as the Lijing River in southern China. Nonetheless, the specific

3 Results

3.1 Vegetation overall promotes carbon capture despite a weak carbon release during the pre-flooding nights

We assume that diel CO_2 flux follows similar patterns as measured on the selected days during the pre-flooding and post-flooding season. Based on this assumption, we compared the diel CO_2 flux of pre-flooding season and post-flooding season. In order to evaluate the effect of vegetation on riparian CO_2 flux, we directly measured the CO_2 fluxes in the riparian area with and without vegetation (bare soil) in different seasons. ~~Because daylight promotes photosynthesis, the first level we reviewed is the diel cycle.~~ Significant diel variations in CO_2 fluxes were observed in the~~terrestrial~~ riparian area in both pre-flooding season (April: low water level before flooding) and post-flooding season (October: resumed low water level after flooding; Table A1). Within a day, the carbon sequestration in the riparian area with vegetation peaked at 10:00 in April and at 14:00 in October (April: -87.89 mg·m^{-2} h^{-1}; October: -104.33 mg·m^{-2} h^{-1}); and the maximum carbon emission occurred at 18:00 (April: 61.49 mg·m^{-2} h^{-1}; October: 34.75 mg·m^{-2} h^{-1}; Fig. 1). However, the time periods that the terrestrial area with vegetation functions as a carbon sink differed in pre-flooding and post-flooding season. In April, carbon sequestration in the riparian area with vegetation was observed between 10:00 to 14:00 hours; while in October, the carbon sequestration was observed between 6:00 to 14:00 hours (Fig. 1). Thus, in post-flooding season, the riparian area with vegetation sequestrated carbon for a longer time. Indeed, the vegetation area's all-day CO_2 flux was 0.358 g·m^{-2} d^{-1} in April but was -0.680 g·m^{-2} d^{-1} in October, transferring from a carbon source to a carbon sink at the daily level. ~~In other words, without submergence, the riparian vegetation may cause more carbon emissions than bare soil at night (than during the day) and function as a carbon source on diel level.~~

Since the flux of vegetation area included fluxes from both soils below and the vegetation above, we subtracted the CO_2 flux of bare soil from the CO_2 flux of vegetation area to measure how the cover of vegetation improve or reduce the carbon sequestration. In April, the difference between area with and without vegetation was 0.128 g·m^{-2} d^{-1}, indicating that vegetation

9
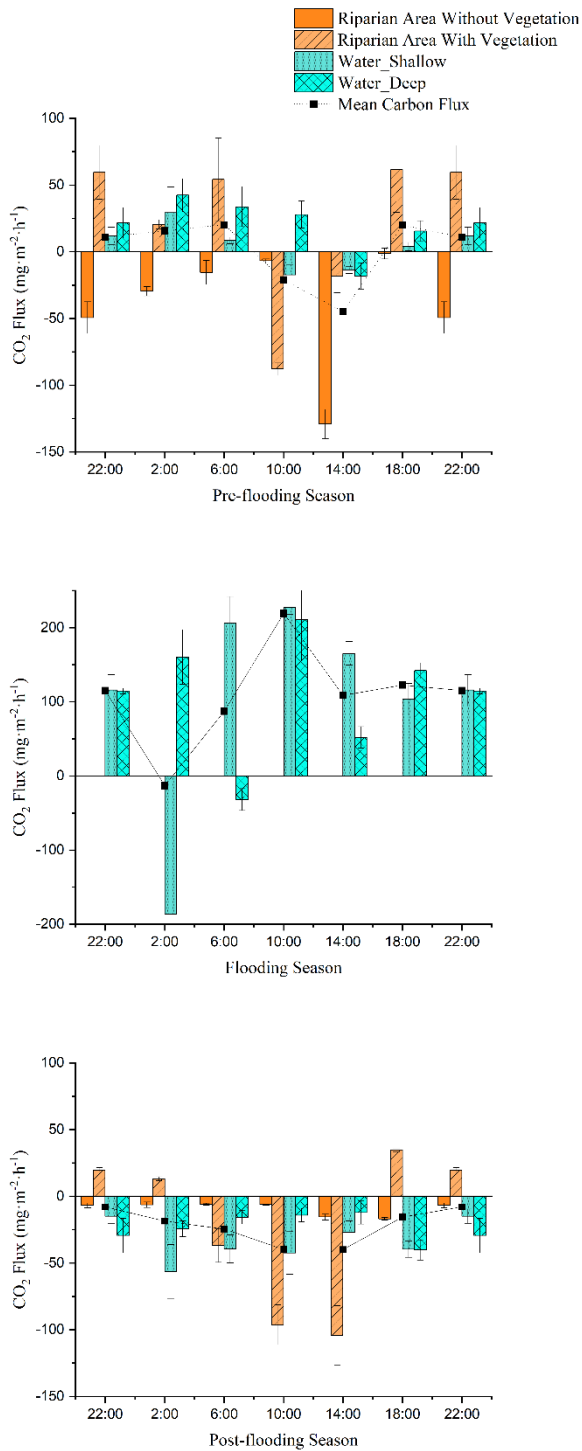
cover actually reduced carbon sequestration and contributed to carbon emission. In October, the difference was -0.453 $g\cdot m^{-2}\, d^{-1}$, indicating that the capacity of vegetation to fix carbon improved after submergence.

The riparian area is composed of vegetation area and bare soil. During the field investigation, we found the vegetation coverage in Lijiang riparian area is about 60%. Using vegetation coverage as the weight, we can get the accumulated CO_2 flux of riparian area (Section 2.2.4, equation(3)). Within a day, the carbon sequestration in the riparian area peaked at 14:00 (April: -62.680 $mg\cdot m^{-2}\, h^{-1}$; October: -68.813 $mg\cdot m^{-2}\, h^{-1}$), and the maximum carbon emission occurred at 18:00 (April: 36.347 $mg\cdot m^{-2}\, h^{-1}$; October: 14.110 $mg\cdot m^{-2}\, h^{-1}$; Fig. 1). In both April and October, the all-day carbon fluxes in the riparian area were negative, indicating that the riparian area acted as a carbon sink in non-flooding season (April: -0.156 $g\cdot m^{-2}\, d^{-1}$, October: -0.500 $g\cdot m^{-2}\, d^{-1}$). The carbon uptake in October, which represented the post-flooding season, was higher. Overall, we found that in the post-flooding season, the riparian vegetation can sequestrate CO_2 for a longer time and fix a higher amount of carbon. Thus, even though the all-day CO_2 flux of bare soil changed from -0.927 $g\cdot m^{-2}\, d^{-1}$ to -0.231 $g\cdot m^{-2}\, d^{-1}$, showing a reduced capacity of carbon sequestration after flooding, the whole riparian area still turned out to be a carbon sink in the post-flooding season.

Figure 1. CO_2 fluxes in riparian area (with vegetation and without vegetation) and fluvial area (shallow and deep) during pre-flooding season (measured in April), flooding season (August), and post-flooding season (October).

3.2 Flooding causes transient carbon emission in fluvial area which turns to sequester carbon during post-flooding season

During the flooding, the riparian areas with and without vegetation were submerged, so only the carbon fluxes from the water-air interfaces were measured (Fig.1b). The water-air CO_2 flux is calculated as the mean of the CO_2 flux in deep water and shallow water considering their coverage is almost half and half. By analysing and calculating the all-day CO_2 flux, we ~~find~~ found that the fluvial area turned from carbon sources in pre-flooding season and during flooding season to a carbon sink in post-flooding season. In 2014 and 2016, the water surface appeared to be carbon sources before and during flooding, with a CO_2 flux ranging from 0.291 g·m^{-2} d^{-1} to 4.678 g·m^{-2} d^{-1} (Fig. 2, Table A2). However, after flooding, the river became a carbon sink (Fig. 2, Table A2). Thus, after flooding, both the riparian area and the fluvial area turned out to be a carbon sink.

Based on the vegetation coverage and the ratio of riparian area width to river width in flooding season, we can accumulate the CO_2 flux of riparian area and the river as a whole (Section 2.2.4). The CO_2 flux of the whole region was 1.833 g·m^{-2} d^{-1} in pre-flooding season, and -0.592 g·m^{-2} d^{-1} in post-flooding season, which indicated that the whole region turned from a carbon source to a carbon sink after flooding.
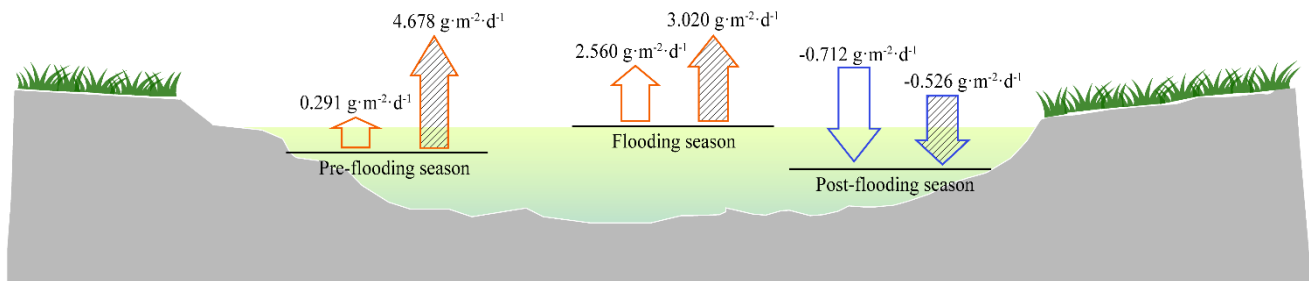
Figure 2. All-day CO_2 flux with low water-level in pre-flooding season, high water-level during flooding season, and resumed low water-level in post-flooding season in 2014 (Blank) and 2016 (Filled). The upward arrow refers to carbon emission, and the downward arrow refers to carbon uptake.

**3.3 Flooding transiently decreases vegetation diversity and promotes the establishment of new dominant species**

Vegetation plays an essential role in the carbon sequestration of riparian area. We hypothesize that the established riparian vegetation species differed, which leads to different vegetation-related carbon fluxes between the pre- and post-flooding periods. We observed that species richness was severely disturbed after flooding. The species richness index decreased from 2.945 in pre-flooding season to 1.695 in post-flooding season (Table 1, Table A3). The dominant species also changed. In pre-flooding season, *Cynodon dactylon* (Linn.) Pers. was dominant, having wide distribution and high coverage in the riparian

11

345 areas. In post-flooding season, *Chrysopogon aciculatus* (Retz.) Trin. (*C. aciculatus*) and *Polygonum lapathifolium* L. were prevalent in surviving species (Table 1). In the 90-day submergence-controlled experiment, *C. aciculatus* also survived, showing good tolerance of flooding submergence, though both individual biomass and the total number of *C. aciculatus* decreased (Fig. 3).

350 **Table 1** The species richness and dominant species change from pre-flooding season to post-flooding season.

	Average species number	Species richness index	Dominant species	Average coverage of dominant species (%)
Pre-flooding	13	2.945	*Cynodon dactylon*	28.61
Post-flooding	7	1.695	*Chrysopogon aciculatus*	28.75

Note: The species number listed here is the average number by plots. The whole list of plant species can be found in Table A3.
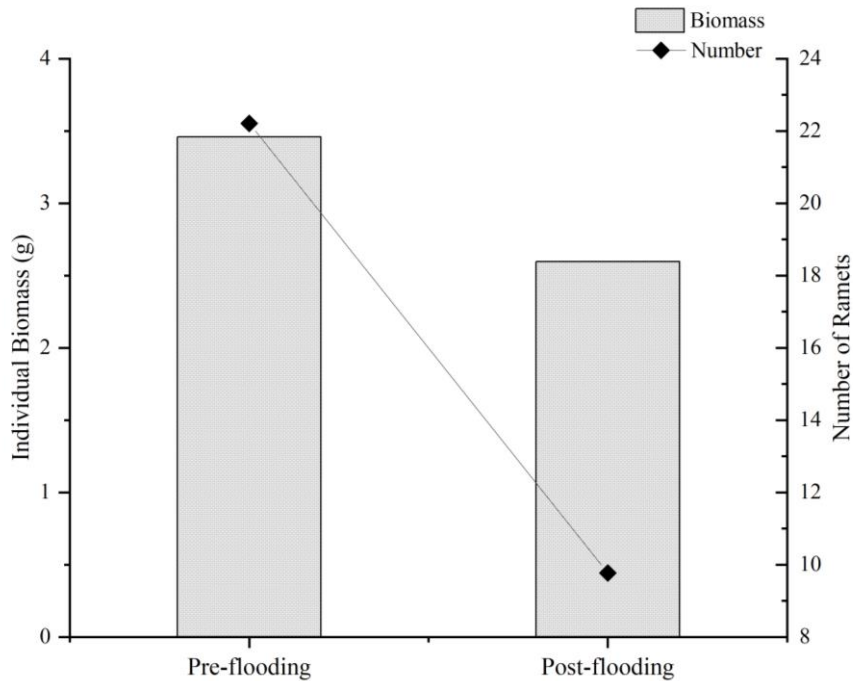
Figure 3. The comparison of the individual biomass and number of *Chrysopogon aciculatus* before and after flooding in the
365 controlled experiment.

3.4 Vegetation density defines carbon sequestration capacity in riparian habitats

We measured total organic carbon (TOC) and total inorganic carbon (TIC) in riparian soils and the fluvial area during different periods. TOC and TIC displayed different patterns across seasons. TOC in fluvial area of the river was substantially higher during the flooding period than that during the pre- and post-flooding seasons (Fig. 4a), probably due to a higher mobilization of riparian organic carbon to the river during the flooding period. This is in consistence with an enrichment effect for organic carbon under high discharge (Raymond and Saiers, 2010). In contrast, TIC in fluvial area of the river was in lower concentration during the flooding period than during the pre- and post-flooding seasons (Fig. 4b). In addition to a dilution effect for TIC by high discharge during the flooding period, this also suggests a stronger effect of riparian area on fluvial carbon during the non-flooding seasons than during flooding periods. Additionally, we show that both TOC and TIC in riparian soils were substantially higher during the post-flooding season than during the pre-flooding season (Fig. 4c, d and Table A4), suggesting a higher carbon sequestration capacity for riparian vegetation after recovery from flooding disturbances.
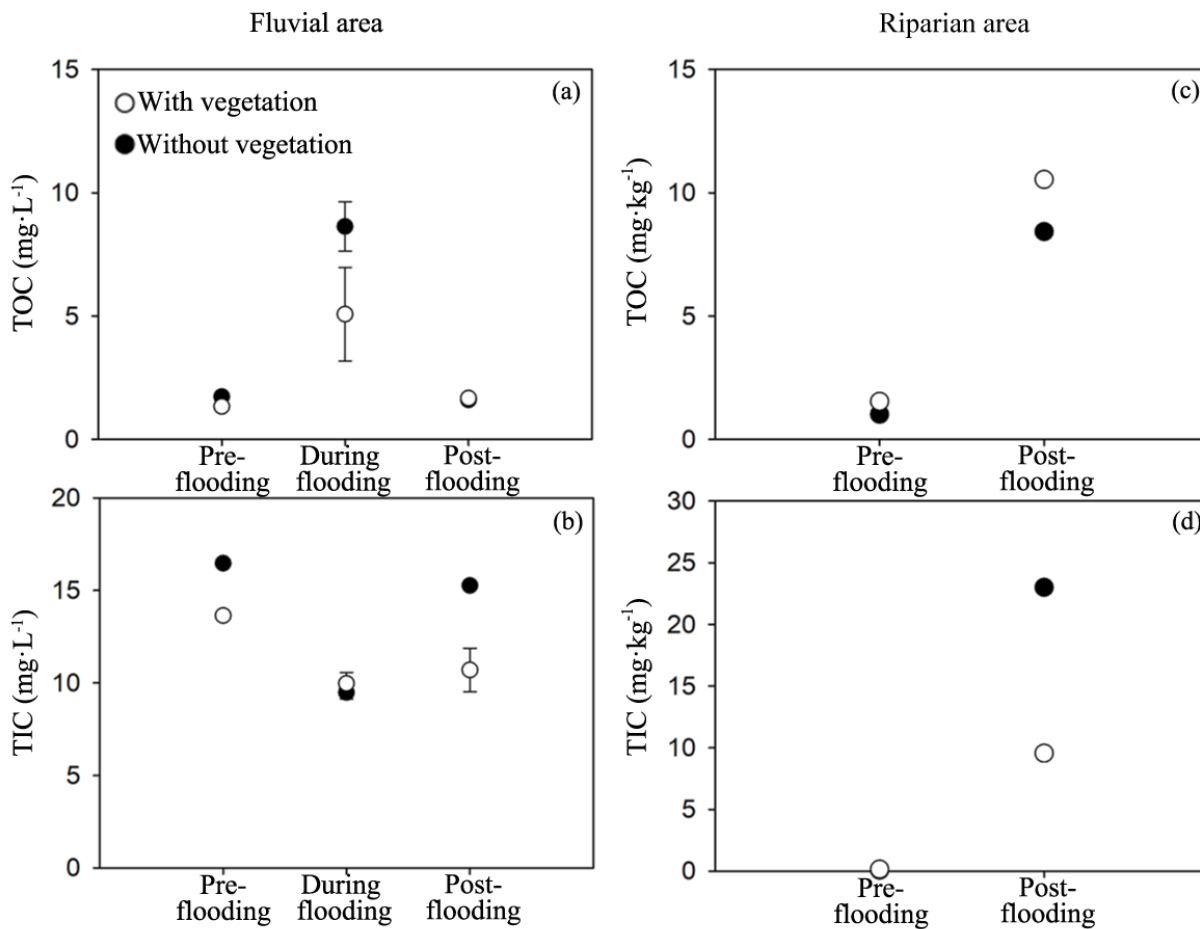
Figure 4. Total organic carbon (TOC) and total inorganic carbon (TIC) in the study area. The aquatic (fluvial area) and riparian habitats (riparian area) include study areas with vegetation and without vegetation. TOC and TIC were also measured in different sampling stages. The ANOVA results for habitats, season, and interaction effects are given, including the degree of freedom (*df*), *F,* and *P* values in Appendix Table A4.

~~**3.5 A carbon offset model shows that Lijiang riparian zones act as carbon sink after flooding but overall, a carbon source**~~

~~Based on the riparian carbon offset model in Sect. 2.3.1, we assume that when *C*=0, the riparian zone would achieve carbon neutralization (Fig. 4). Under the assumption of carbon neutralization, the relationship between the flooding days and the post-disturbance vegetation coverage required to achieve carbon neutralization can be revealed. For example, using the carbon flux measured in Lijiang River in this study, we found that the riparian zone can only achieve carbon neutralization when flooding days are fewer than 15 days, assuming the post-disturbance vegetation coverage in the dry season is about 60%. Since the flooding season can hardly be only 15 days, the Lijiang riparian zone is overall a carbon source at the yearly level and cannot reach carbon neutralization. This is mainly due to the high carbon emission during flooding. The flooding days in Lijiang River are about 80 days, assuming the river width is 175m and the vegetation coverage to be 60%, the net CO_2 flux in Lijiang River is 35.75 kg·m⁻¹·year⁻¹. Though the recovered vegetation help fix 3.29 kg·m⁻¹ more CO_2 after flooding, the carbon emission during the flooding season achieves 39.06 kg·m⁻¹. Also, besides the contribution of recovered vegetation, our data shows that bare soil also contributes to the carbon neutralization, but the mechanism for bare soil to capture carbon still needs further soil chemistry analysis. Flooding days and post-flooding days are also essential factors for the carbon offset model, future detailed measurements are required to monitor the carbon dynamics of the riparian zone.~~
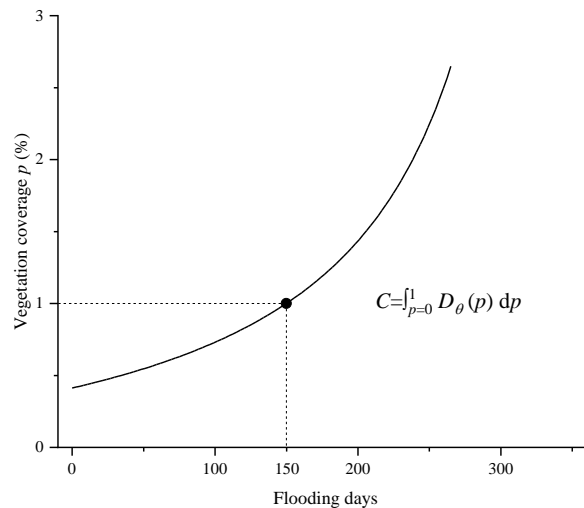

14

3.6 Disturbance in riparian zones significantly contributes to global carbon sequestration

After flooding disturbance, the riparian water surface becomes a carbon sink from a carbon source with a CO_2 flux of -0.62 g·m^{-2}·d^{-1}, about 1.58 times the CO_2 flux of global forests (-0.39 g·m^{-2}·d^{-1}) (Harris et al., 2021). The riparian zone has a higher efficiency in capturing CO_2 than forests. The global CO_2 fixed by river after flooding disturbance reaches 0.11 Gt per year. After flooding disturbance, the water surface of riparian zone fixs 0.53 Gt more CO_2 compared with pre-flooding season, which is about 9.1 % of the CO_2 fixed by the global forests. Proper restoration of the riparian zone after flooding disturbance can greatly contribute to global carbon offset (Fig. 5).
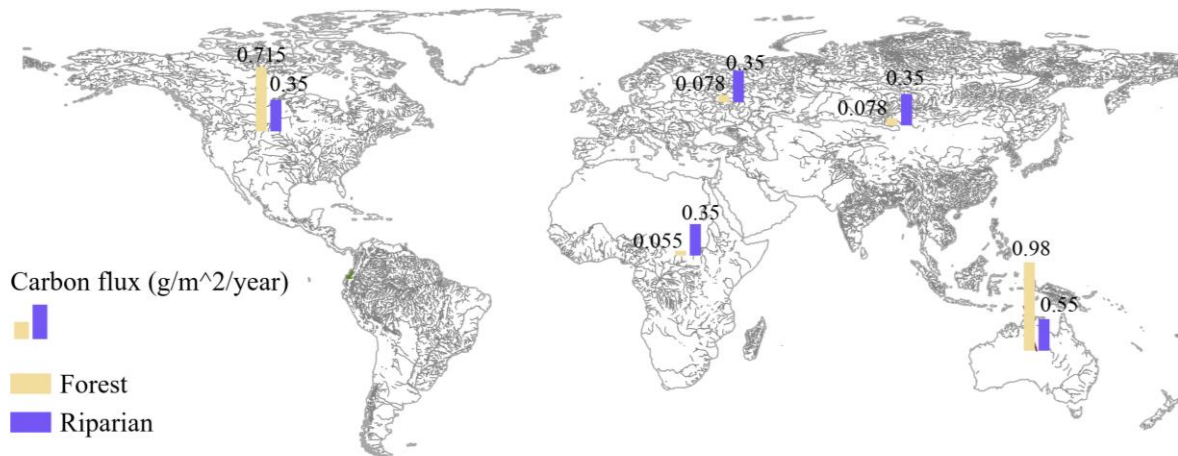

Figure 5. Carbon fluxes in forests and riparian zones of Asia, North America, Europe, Africa, and Australia. The riparian carbon flux for each continent is estimated by data collected in this study. Combining the riparian carbon flux data with flooding days, days of winter and fall, and continental riparian area, one can calculate the total carbon flux for each continent. The forest carbon flux is collected from previously published papers and authoritative online resources. The riparian carbon flux is higher than forest carbon flux in Asia, Europe, and Africa, showing great potential in carbon offset.

15

4 Discussion

The present work demonstrates significant variations in spatial and temporal carbon fluxes from riparian zones of the Lijiang River. In April, the all-day CO_2 fluxes in 2014 and 2016 were positive on the daily scale in aquatic habitat, indicating a net emission from fluvial area of the river to the atmosphere. However, opposite results were found for the CO_2 flux in October after the flooding disturbance, which was negative and indicated a capacity for carbon sequestration. In the riparian area, the vegetation was found to promote the overall carbon sequestration and keep the riparian area as a carbon sink. It demonstrates that the carbon sequestration capacity of a given system depends strongly on the post-disturbance recovery of riparian vegetation.

4.1 Increased carbon emission during flooding periods of the riparian zone

Hydrological flow has been found to be an essential factor within the carbon cycle of riparian ecosystems (Zarnetske et al., 2018). Our data suggest that flooding not only affects carbon emission from the fluvial channel but also the carbon fluxes of the riparian area. With regard to carbon emission from the fluvial channel, our data show that carbon emission of water-air interface significantly increased and showed a net emission of CO_2 in both the daytime and night-time (all-day CO_2 flux: 0.291 $g \cdot m^{-2} d^{-1}$ in April, 2.560 $g \cdot m^{-2} d^{-1}$ in August). This is probably due to the increased lateral carbon flux from terrestrial areas to rivers due to flooding. Research found that when water flows through ecosystem, it would pick up dissolved organic carbon from vegetation and soils, transporting the carbon from riparian ecosystem to streams (Raymond and Saiers, 2010). A large amount of carbon could be transported to the river because of enhanced hydrological connectivity between the fluvial channel and its riparian areas during flooding periods (Zarnetske et al., 2018).

When comparing the CO_2 flux of shallow-water area (with aquatic vegetation) and deep-water area (without vegetation) (Fig. A2), it is also found that shallow-water released less carbon in pre-flooding season and captured more carbon in post-flooding season than deep-water area (pre-flooding: 0.090 $g \cdot m^{-2} d^{-1}$ in shallow water, 0.492 $g \cdot m^{-2} d^{-1}$ in deep water; post-flooding: -0.880 $g \cdot m^{-2} d^{-1}$ in shallow water, -0.545 $g \cdot m^{-2} d^{-1}$ in deep water). However, during the flooding season, both the shallow-water and deep-water areas had a carbon flux of about 2.55 $g \cdot m^{-2} d^{-1}$, probably because of an enhanced input of carbon from riparian vegetation and soils to the waters.

In addition to increased hydrologic connectivity between the riparian area and fluvial channel of the river, enhanced carbon emission also results from enhanced substrate availability during flooding (Hirota et al., 2007). Previous work also reported that the extensive root system of riparian species with strong taproots and well-developed fibrous roots could force the species to demand more oxygen and accelerate root respiration and CO_2 emissions from the neighbouring rhizosphere (Elias et al., 2015). In submerged areas, the CO_2 may be transported to water and then released to the atmosphere as the carbon flux of water surface. Especially, the recovery of some C_4 riparian species after periodic flooding also contributed to the higher gas

16

460 transportability and abundant substrate for CO_2 emission compared to the performance of C_3 species (Still et al., 2003). In addition to riparian vegetation, inundation could also increase the decomposition of stored organic matter (Denef *et al.*, 2001, Marín-Muñiz *et al.*, 2015) and soil respiration (Anderson *et al.*, 2020, Ou *et al.*, 2019). A previous study found that after 25 days of soil moisture enhancement, the anaerobiosis stimulates CO_2 loss by 1.5 times more than the normal soil moisture environment (Huang & Hall, 2017). Flooding leads to elevated soil moisture for weeks or even months, and thus an accelerated
465 CO_2 supply to the inundated channel.

4.2 Post-disturbance survived vegetation as a critical factor for riparian systems to sequester carbon

We observed that the carbon sequestration of riparian area and fluvial area as a whole was greatly enhanced after the flooding period, to the point that the overall carbon flux was negative. In consistence with our analysis, Kathilankal et al. (2008)
470 proposed that tidal inundation caused a mean reduction of 49 % in the marsh-atmosphere carbon (CO_2) flux compared to non-flooded conditions (Kathilankal *et al.*, 2008). Our study offers proof that the hydrological flow is a determining factor on whether the riparian ecosystem is a net carbon source or sink.

One possible reason is that the vegetation's recovery after flooding enhances its ability to sequester more CO_2 for
475 photosynthesis. The post-flooding succession of vegetation suggests that not all riparian plants can survive submergence and to become efficient carbon sinks. Indeed, species richness decreased after flooding, which indicates a decrease of the interspecific competition, giving a chance to species that can quickly recover from submergence. The dominant species changed from *C. dactylon* to *C. aciculatus* after flooding disturbance. Although the individual biomass and number of *C. aciculatus* did not increase, existing literature suggests that the leaf maximum net photosynthesis rate may increase
480 significantly after severe submergence in the riparian zones of Lijiang (Huang *et al.*, 2017, Jie *et al.*, 2012). For the clonal plants, its physiological integration allowing them to survive submergence and spread rapidly after de-submergence. Luo et al. (2014), studying *Alternanthera philoxeroides* (alligator weed) after 30 days of submergence, found that connections between submerged and non-submerged ramets enhance the performance of the submerged ramets; and the de-submerged ramets had high soluble sugar concentrations, suggesting high metabolic activities (Luo et al., 2014). Wei et al. (2018) also found that
485 after 30 days of submergence, stolon connection significantly increased growth, biomass allocation to roots and photosynthetic capacities of the submerged ramets, and increased growth and photosynthetic capacities of the unsubmerged ramets (Wei et al., 2018). Also, flooding could promote CO_2 use efficiency and the ability of the plant to use low light (Wang et al., 2019a). The enhanced photosynthetic capacity is believed to be one of the physiological strategies for species growing in critical zones with flooding disturbance. Moreover, human impacts can no longer be ignored on the riparian ecosystem (Ren et al., 2019),
490 suggesting vegetation that can recover quickly and densely is essential to allow riparian zones to be efficient carbon sinks.

Our results suggest, on an annual scale, riparian area behaves either as a net source or sink of carbon depending on the relative importance between enhanced emission during flooding and the strength of post-disturbance carbon absorbance. Assuming the carbon flux rates of flooding season and non-flooding seasons were the same as we have measured on the selected days (Section 2.2.4, Fig.1-2), we estimated that the riparian area and the fluvial area as a whole can achieve carbon neutralization (C_{annual}=0) only when flooding days are fewer than 15 days. Therefore, the relative ratio of flooding to non-flooding days are essential factors to determine whether the riparian area is a net source or sink on an annual scale, and future long-term, high-frequency measurements are required to monitor the carbon dynamics of the riparian zone. Also, besides the contribution of recovered vegetation, our data shows that bare soil also contributes to the carbon neutralization, but the mechanism for bare soil to capture carbon still needs further analysis.

Nowadays, the risk and the number of global flooding events are expected to rise significantly with global warming (Hirabayashi et al., 2013). This means that the annual carbon cycle of riparian area and fluvial area as a whole is subject to a more variant and stronger impact from flooding. Previous research found that with a warmer climate, there would be a large increase in flood frequency in Southeast Asia, Peninsular India, eastern Africa and the northern half of the Andes (Hirabayashi et al., 2013). Our research highlights that flooding disturbance would not only cause large carbon emission during the flooding season, but can also promote carbon sequestration in the post-flooding season. It is therefore necessary to consider the dynamic effect of flooding on ecosystems' carbon cycle especially under global climate change.

4.1 Post-disturbance survived vegetation is a critical factor that allows riparian systems to change from carbon source to carbon sink after flooding

We observed that the carbon sequestration of riparian zone was greatly enhanced after the flooding period, to the point that the overall carbon flux was negative. Kathilankal et al. (2008) also proposed that tidal inundation caused a mean reduction of 49 % in the marsh atmosphere carbon (CO_2) flux compared to non-flooded conditions (Kathilankal *et al.*, 2008). Our study offers proof that the hydrological flow is a determining factor on whether the ecosystem is a net carbon source or sink. One possible reason is that the vegetation's recovery after flooding enhances its ability to sequestrate more CO_2 for photosynthesis. Still, the succession of vegetation we observed after flooding suggests that not all plants can survive submergence and to be as efficient as carbon sinks. Indeed, species richness decreased after flooding, which indicates a decrease of the interspecific competition, giving a chance to species that can quickly recover from submergence. The dominant species changed from *C. dactylon* to *C. aciculatus* after flooding disturbance. Although the individual biomass and number of *C. aciculatus* do not increase, existing literature suggests that the leaf maximum net photosynthesis rate may increase significantly after severe submergence in the riparian zones of Lijiang (Huang *et al.*, 2017, Jie *et al.*, 2012). For the clonal plants, its physiological integration allowing them to survive submergence and spread rapidly after de-submergence. Luo et al. (2014), studying *Alternanthera philoxeroides* (alligator weed) after 30 days of submergence, found that connections between submerged and

18

non-submerged ramets enhance the performance of the submerged ramets; and the de-submerged ramets had high soluble sugar concentrations, suggesting high metabolic activities (Luo et al., 2014). Wei et al. (2018) also found that after 30 days of submergence, stolon connection significantly increased growth, biomass allocation to roots and photosynthetic capacities of the submerged ramets, and increased growth and photosynthetic capacities of the un-submerged ramets (Wei et al., 2018). Also, flooding could promote CO_2 use efficiency and the ability of the plant to use low light (Wang et al., 2019a). The enhanced photosynthetic capacity is believed to be one of the physiological strategies for species growing in critical zones with flooding disturbance. Moreover, human impacts can no longer be ignored on the riparian ecosystem (Ren et al., 2019), suggesting vegetation that can recover quickly and densely is essential to allow riparian zones to be efficient carbon sinks.

Our data also shows that vegetation land before flooding can be a carbon source. This perhaps because the role of vegetation as a substrate source through litter production and root exudates can vary among species (Hirota et al., 2007). Previous work also reported that the extensive root system of riparian species with strong taproots and well-developed fibrous roots could force the species to demand more oxygen and accelerate root respiration and CO_2 emissions from the neighbouring rhizosphere (Elias et al., 2015). In submerged areas, the CO_2 may be emitted to water and then released to the atmosphere as the carbon flux of water surface. Especially, the recovery of some C_4 riparian species after periodic flooding also contributed to the higher gas transportability and abundant substrate for CO_2 emission compared to the performance of C_3 species (Still et al., 2003). Research should be directed towards understanding how plants such as *C. aciculatus* can colonize flooded riparian zones efficiently and promoting plants with similar characteristics in restoration efforts.

When comparing the CO_2 flux of shallow-water area (with aquatic vegetation) and deep-water area (with no vegetation) (Fig. A3), it is also found that shallow-water releases less carbon in pre-flooding season and captures more carbon in post-flooding season than deep-water area (pre-flooding: 0.090 g·m^{-2}·d^{-1} in shallow water, 0.492 g·m^{-2}·d^{-1} in deep water; post-flooding: 0.880 g·m^{-2}·d^{-1} in shallow water, 0.545 g·m^{-2}·d^{-1} in deep water). However, during the flooding season, both the shallow-water and deep-water areas have carbon flux of about 2.55 g·m^{-2}·d^{-1}, probably because during flooding no aquatic vegetation was able to fix carbon through photosynthesis.

4.2 Flooding disturbance leads to transiently increasing carbon emission, which cannot be offset by post-disturbance recovery

During the flooding period, the carbon emission of water area significantly increases and shows a net emission of CO_2 in both the daytime and night time (all-day CO_2 flux: 0.291 g·m^{-2}·d^{-1} in April, 2.560 g·m^{-2}·d^{-1} in August). This is probably due to the increased lateral carbon flux from terrestrial areas to rivers due to flooding. Research found that when water flows through ecosystem, it would pick up dissolved organic carbon (DOC) from vegetation and soils, transporting DOC from terrestrial ecosystem to streams. When the water is flowing fast, more carbon would be transported out of the watersheds. Zarnetske et al. (2018) found that in 80% of the watersheds of United States the hydrologic flow determined the DOC flux behaviour (Zarnetske et al., 2018).

Using the carbon offset model, the result shows that even with 100% vegetation coverage, the whole riparian zone can hardly achieve carbon neutralization at yearly level when the flooding days are higher than 15. This is mainly due to the high

carbon emission during flooding. Nowadays, with global warming, the risk and the number of global flooding events are also rising (Hirabayashi et al., 2013), meaning that the carbon cycle of riparian zone are more dynamic than ever. Based on 11 climate models, previous research projects found that with a warmer climate, there would be a large increase in flood frequency in Southeast Asia, Peninsular India, eastern Africa and the northern half of the Andes (Hirabayashi et al., 2013). Our research highlights that flooding disturbance would not only cause large carbon emission during the flooding season, but can also promote carbon sequestration in the post-flooding season. It is necessary to consider the dynamic effect of flooding on ecosystems' carbon cycle especially under global climate change. 4.3 Microbial and abiotic contributions to carbon capture in riparian zones While our research suggests that vegetation is a major factor in defining carbon fluxes, microbial organisms likely bring a significant contribution to our results, too. The carbon sequestration of bare soil decreased from pre-flooding season to post-flooding season. It can be attributed to the fact that inundation periods increases soil enzyme activities (Geng *et al.*, 2017, Ou *et al.*, 2019), active bacterial counts, and respiration rates (Anderson *et al.*, 2020, Ou *et al.*, 2019). The aerobic conditions during wet-dry cycles could increase the decomposition of stored organic matter in soils (Denef *et al.*, 2001, Marín-Muñiz *et al.*, 2015). A previous study found that after 25 days of soil moisture enhancement, the anaerobiosis stimulates CO_2 loss by 1.5 times more than the normal soil moisture environment (Huang & Hall, 2017). Flooding leads to elevated soil moisture for weeks or even months, and thus the bare soil after flooding may show an accelerated CO_2 emission.

4.4 Riparian zones are seasonal areas of high carbon capture

Hydrological flow has been found to be an essential factor within the carbon cycle of various ecosystems (Zarnetske et al., 2018). Our data confirms this, as discussed in both Sect. 4.1 and Sect. 4.2. It would influence not only the river carbon emission but also the terrestrial carbon emission. The water flow and terrestrial vegetation combined making the riparian zone a dynamic carbon pool.

After flooding disturbance, the riparian zone turns from a carbon source to a carbon sink mainly due to vegetation's increased CO_2 capture efficiency and river's also capturing carbon. Though riparian zone is found to be a carbon source in both pre- and post-flooding seasons, with flooding disturbance, the riparian zone has a chance to achieve carbon neutralization at a yearly level. Based on the carbon offset model, we can evaluate the annual CO_2 flux of the riparian zone and evaluate the potential for a certain riparian zone to be a carbon sink. The post-disturbance riparian zone shows huge potential in carbon capture compared with global forest, which is a large and persistent carbon sink with an annual magnitude of 2.4 ± 0.4 Gt C yr^{-1} (Pan et al., 2011). After considering the emissions of forest degradation, the global forest-atmosphere CO_2 flux is estimated to be -5.8 Gt CO_2 yr^{-1} (Harris et al., 2021). Global riparian zone after flooding disturbance, with an estimated global area of 468,000 km^2, can fix up to 0.53 Gt more CO_2. It is larger than the net carbon flux in the rainforest in the Amazon river basin (0.10 CO_2e Gt per year) (Harris et al., 2021). Additionally, the riparian zone after flooding disturbance was found to have a higher carbon sequestration efficiency, which is consistent with previous research (Hastie *et al.*, 2019). Its daily average CO_2 flux is -0.57 g m^{-2} d^{-1} (water: -0.62 g m^{-2} d^{-1}, terrestrial area: -0.455 g m^{-2} d^{-1} without vegetation; -0.680 g m^{-2} d^{-1} with vegetation), while the forest is -0.39 g m^{-2} d^{-1} (Harris et al., 2021).

20

Many have discussed the diel variability of CO_2 flux in the riparian zone (Gómez-Gener et al., 2021; Reiman and Xu, 2019). Yet, few studies considered the positive effects of flooding season on the carbon cycle and may overestimate the CO_2 emissions. Previous research has found that the nocturnal CO_2 emissions are on average 27% (0.9 gC m^{-2} d^{-1}) greater than those estimated from diurnal concentrations alone (Gómez-Gener et al., 2021). Ignoring night-time CO_2 emissions may underestimate global estimates of carbon emission from running waters to the atmosphere by 0.20–0.55 PgC yr^{-1} (Gómez-Gener et al., 2021). Tiegs et al. 2019 found that the biomes in riparian zones have distinct carbon processing signatures around the earth, but they mainly analysed sites that are relatively free of human impacts (Tiegs et al., 2019).

5 Conclusions

Under global warming, both the risk and the number of flooding event are rising. Our analysis reinforces the need to consider post-disturbance recovered vegetation in riparian zone as a climate mitigation strategy. The recovery of survived riparian vegetation from flooding disturbance can limit overall carbon emission and help neutralize the carbon emissions caused by flooding. Flooding also improves the resource hunting ability of water area, which turns the riparian zone from a carbon source to a carbon sink. 0.53 Gt year^{-1} more CO_2 is captured because of the flooding, which is 9.1 % of the total CO_2 flux of global forest. This study highlights that carbon-conscious conservation efforts in post-flooding season should promote the establishment of high densities of specific plant species that are both flooding-resistant and efficient at capturing carbon.

Appendix A
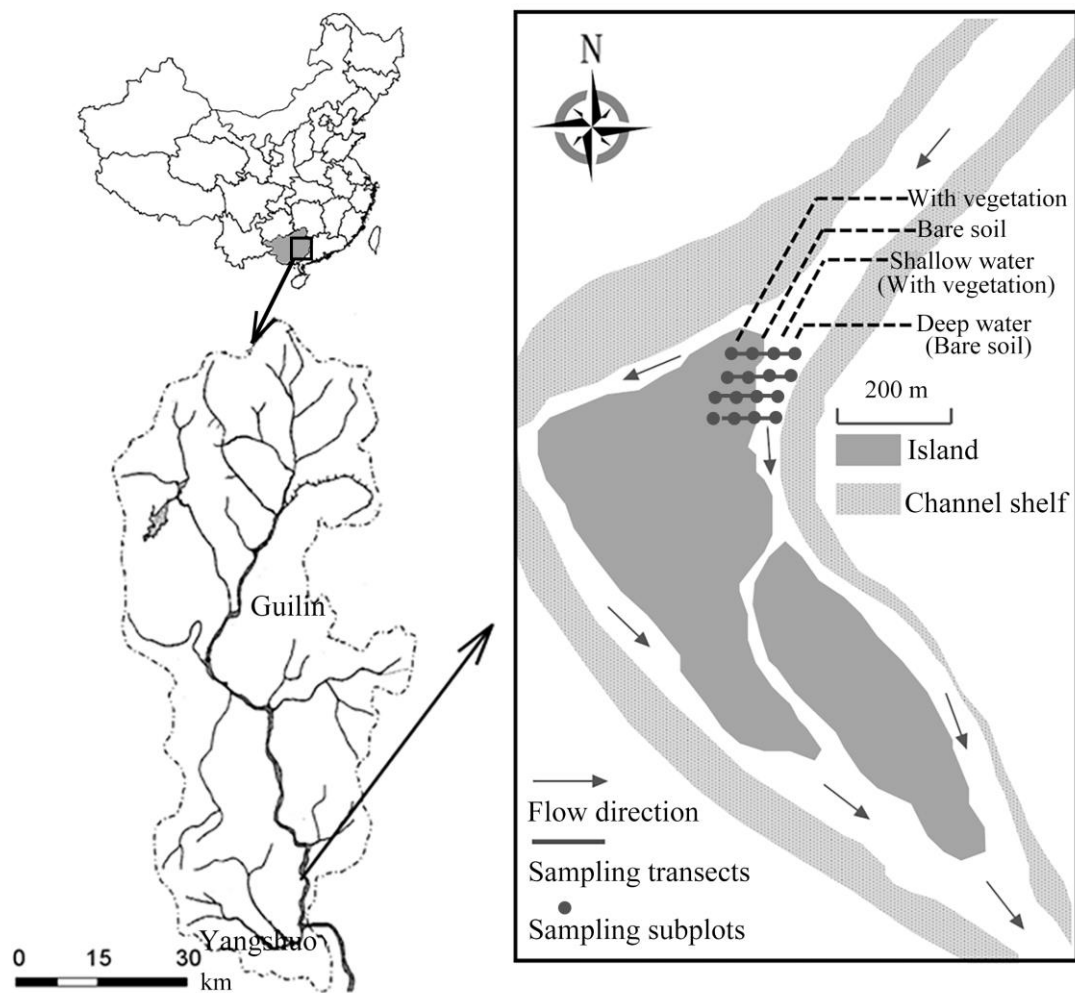
610 **Appendix Figure A1:** The location of the study site in the island downstream of Lijiang River in Guilin city, southwest China (25° 06′ N, 110° 25′ E). There were four sampling transects (black lines), each spaced 3 m, and four subplots (black squares) were arranged in each transect, with the distance of 5-8 m between each other.
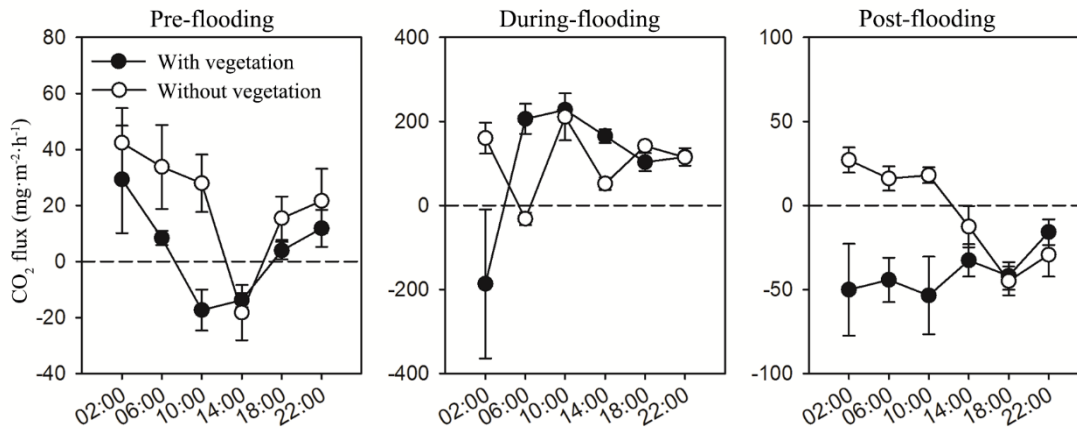
615

Appendix Figure A2: Effects of time (measuring times in one day) on CO_2 flux in the water surface of the water sections with vegetation (shallow-water, filled) and without vegetation (deep-water, blank) in the three sampling stages. Mean $\pm$ 1 SE is given.

620 **Appendix Table A1.** Repeated measurements ANOVA for effects of vegetation (bare soil without vegetation vs. with vegetation; between-subject factor) and time (measuring times in one day; within-subject factor) on the CO_2 fluxes in two sampling stages (April and October) in terrestrial habitats. Degree of freedom, F, and P (significance) values.

Sampling stages	Effects	df	F	p-value
April	Vegetation (V)	1,8	**102.506**	**<0.001**
	Time (T)	5,40	**22.411**	**<0.001**
	T x V	5,40	**12.909**	**<0.001**
October	Vegetation (V)	1,8	**61.47**	**<0.001**
	Time (T)	5,40	**9.25**	**<0.001**
	T x V	5,40	**5.959**	**<0.001**

F value: the ratio of two estimates of the variance between or within groups in ANOVAs;

P-value: the probability of the F value in the F distribution. The p-values were calculated under the null hypothesis that CO_2

625 flux is not influenced by the existence of grass or measuring times in terrestrial habitats.

Appendix Table A2. Repeated measurements ANOVA for effects of sampling position (water surface with vegetation vs. without vegetation; between-subject factor) and time (measuring times in one day; within-subject factor) on CO_2 fluxes in three sampling stages (April, August, and October) in aquatic habitats. Degree of freedom (*df*), F, and P (significance) values are given.

Sampling stages	Effects	*df*	F	p-value

April	Position (P)	1,4	0.003	0.956
	Time (T)	5,20	**4.306**	**0.008**
	T x P	5,20	**7.431**	**<0.001**
August	Position (P)	1,4	0.003	0.956
	Time (T)	5,20	**4.306**	**0.008**
	T x P	5,20	**7.431**	**<0.001**
October	Position (P)	1,4	7.484	0.052
	Time (T)	5,20	2.183	0.097
	T x P	5,20	**6.552**	**0.001**

630 *F* value: the ratio of two estimates of the variance between or within groups in ANOVAs; *P*-value: the probability of the *F* value in *F* distribution. The *p*-values were calculated under the null hypothesis that CO_2 flux is not influenced by sampling positions or measuring times in aquatic habitats.

Appendix Table A3. The whole plant species in pre-flooding season (surveyed in April) and post-flooding season (surveyed

635 in October).

Pre-flooding season	Post-flooding season
Aster tataricus	*Alternanthera philoxeroides*
Astragalus sinicus	*Aster tataricus*
Athyrium sinense	*Astragalus sinicus*
Cardamine hirsuta	*Cardamine hirsuta*
Carex duriuscula subsp. *stenophylloides*	*Carex polycephala* var. simplex
Carex polycephala var. simplex	*Chrysopogon aciculatus*
Chrysopogon aciculatus	*Cynodon dactylon*
Cichorium endivia	*Oxalis corymbosa*
Conyza canadensis	*Polygonum hydropiper*
Cynodon dactylon	*Polygonum lapathifolium*
Digitaria ciliaris	*Stellaria media*
Hemarthria altissima	
Lindernia antipoda	
Oxalis corymbosa	
Poa annua	
Polygonum hydropiper	
Polygonum lapathifolium	
Polygonum muricatum	
Potentilla chinensis	
Salvia plebeia	

24

Stellaria media
Urena lobata
Viola philippica
Vitex negundo

Appendix Table A4 ANOVA results for effects of vegetation (with vegetation vs. without vegetation; between-subject factor), sampling seasons (pre-flooding, during flooding, post-flooding), and interaction effects on total organic carbon (TOC) and total inorganic carbon (TIC) in two positions (fluvial area vs. riparian area). Degree of freedom (*df*), *F,* and *P* (significance) values are given.

	Fluvial area				Riparian area			
	TOC		TIC		TOC		TIC	
	$F_{1,8}$	*P*	$F_{1,8}$	*P*	$F_{1,8}$	*P*	$F_{1,8}$	*P*
Habitat	3.3	0.094	25.8	<0.001	116.8	<0.001	2289.3	<0.001
Season	24.2	<0.001	46.6	<0.001	4515.9	<0.001	13360.4	<0.001
Interaction	2.5	0.0120	10.7	<0.001	42.8	<0.001	2336.7	<0.001

Author contributions

RL conceived, designed the study and collected the data with FY. YZ analysed the data, completed data visualization. YZ and RL wrote the original manuscript. HZ, SL, TGG reviewed and edited the manuscript. HZ acquired funding and resources for this study.

Competing interests

The authors declare that they have no conflict of interest.

Disclaimer

Publisher's note: Copernicus Publications remains neutral with regard to jurisdictional claims in published maps and institutional affiliations.

References

Agilent Technologies: User Manuals Agilent 7890A Gas Chromatograph Operating Guide, 2010.

660 Allen, D. E., Dalal, R. C., Rennenberg, H., Meyer, R. L., Reeves, S., and Schmidt, S.: Spatial and temporal variation of nitrous oxide and methane flux between subtropical mangrove sediments and the atmosphere, Soil Biology and Biochemistry, 39, 622–631, https://doi.org/10.1016/j.soilbio.2006.09.013, 2007.

Anderson, N. J., Heathcote, A. J., Engstrom, D. R., and Globocarb data contributors: Anthropogenic alteration of nutrient supply increases the global freshwater carbon sink, Sci. Adv., 6, eaaw2145, https://doi.org/10.1126/sciadv.aaw2145, 2020.

665 Bullock, J. M., Aronson, J., Newton, A. C., Pywell, R. F., and Rey-Benayas, J. M.: Restoration of ecosystem services and biodiversity: conflicts and opportunities, Trends in Ecology & Evolution, 26, 541–549, https://doi.org/10.1016/j.tree.2011.06.011, 2011.

Colmer, T. D., Voesenek, L. a. C. J., Colmer, T. D., and Voesenek, L. a. C. J.: Flooding tolerance: suites of plant traits in variable environments, Functional Plant Biol., 36, 665–681, https://doi.org/10.1071/FP09144, 2009.

670 Darrel Jenerette, G. and Lal, R.: Hydrologic sources of carbon cycling uncertainty throughout the terrestrial-aquatic continuum, Global Change Biol, 0, 1873–1882, https://doi.org/10.1111/j.1365-2486.2005.01021.x, 2005.

Dybala, K. E., Matzek, V., Gardali, T., and Seavy, N. E.: Carbon sequestration in riparian forests: A global synthesis and meta-analysis, Global Change Biology, 25, 57–67, https://doi.org/10.1111/gcb.14475, 2019.

Dynesius, M. and Nilsson, C.: Fragmentation and Flow Regulation of River Systems in the Northern Third of the World, 675 Science, 266, 753–762, https://doi.org/10.1126/science.266.5186.753, 1994.

Elias, E., Steele, C., Havstad, K., Steenwerth, K., Chambers, J., Deswood, H., Kerr, A., Albert, R., Schwartz, M., Stine, P., and Steele, R.: Southwest Regional Climate Hub and California Subsidiary Hub assessment of climate change vulnerability and adaptation and mitigation strategies, 2015.

Gaughan, A. E. and Waylen, P. R.: Spatial and temporal precipitation variability in the Okavango–Kwando–Zambezi
680 catchment, southern Africa, Journal of Arid Environments, 82, 19–30, https://doi.org/10.1016/j.jaridenv.2012.02.007, 2012.

Gregory, S. V., Swanson, F. J., McKee, W. A., and Cummins, K. W.: An Ecosystem Perspective of Riparian Zones, BioScience, 41, 540–551, https://doi.org/10.2307/1311607, 1991.

Hassanzadeh, Vidon, Gold, Pradhanang, and Lowder: RZ-TRADEOFF: A New Model to Estimate Riparian Water and Air Quality Functions, Water, 11, 769, https://doi.org/10.3390/w11040769, 2019.

685 Hirabayashi, Y., Mahendran, R., Koirala, S., Konoshima, L., Yamazaki, D., Watanabe, S., Kim, H., and Kanae, S.: Global flood risk under climate change, Nature Clim Change, 3, 816–821, https://doi.org/10.1038/nclimate1911, 2013.

Hirota, M., Senga, Y., Seike, Y., Nohara, S., and Kunii, H.: Fluxes of carbon dioxide, methane and nitrous oxide in two contrastive fringing zones of coastal lagoon, Lake Nakaumi, Japan, Chemosphere, 68, 597–603, https://doi.org/10.1016/j.chemosphere.2007.01.002, 2007.

690 Hondula, K. L., Jones, C. N., and Palmer, M. A.: Effects of seasonal inundation on methane fluxes from forested freshwater wetlands, Environ. Res. Lett., 16, 084016, https://doi.org/10.1088/1748-9326/ac1193, 2021.

Huang, D., Wang, D., Ren, Y., Qin, Y., and Wu, L.: Responses of leaf traits to submergence stress and analysis of the economic spectrum of plant species in an aquatic-terrestrial ecotone, the Li River, Acta Ecol. Sin., 37, http://dx.doi.org/10.5846/stxb201508281789, 2017.

695 Le Mer, J. and Roger, P.: Production, oxidation, emission and consumption of methane by soils: A review, European Journal of Soil Biology, 37, 25–50, https://doi.org/10.1016/S1164-5563(01)01067-6, 2001.

Li, X., Shi, F., Ma, Y., Zhao, S., and Wei, J.: Significant winter CO_2 uptake by saline lakes on the Qinghai-Tibet Plateau, Global Change Biology, 28, 2041–2052, https://doi.org/10.1111/gcb.16054, 2022.

Liu, R., Liang, S., Long, W., and Jiang, Y.: Variations in Leaf Functional Traits Across Ecological Scales in Riparian Plant
700 Communities of the Lijiang River, Guilin, Southwest China, trcs, 11, https://doi.org/10.1177/1940082918804680, 2020.

Liu, X., Lu, X., Yu, R., Sun, H., Xue, H., Qi, Z., Cao, Z., Zhang, Z., and Liu, T.: Greenhouse gases emissions from riparian wetlands: an example from the Inner Mongolia grassland region in China, Biogeosciences, 18, 4855–4872, https://doi.org/10.5194/bg-18-4855-2021, 2021.

Lu, Y. and Wang, D.: Diversity of plants on the Alluvial islands of Lijiang River basin and the physicochemical properties of
705 their soil, Nature Environment and Pollution Technology, 14, 533–540, 2015.

Luo, F.-L., Chen, Y., Huang, L., Wang, A., Zhang, M.-X., and Yu, F.-H.: Shifting effects of physiological integration on performance of a clonal plant during submergence and de-submergence, Annals of Botany, 113, 1265–1274, https://doi.org/10.1093/aob/mcu057, 2014.

Maraseni, T. N. and Cockfield, G.: Crops, cows or timber? Including carbon values in land use choices, Agriculture,
710 Ecosystems & Environment, 140, 280–288, https://doi.org/10.1016/j.agee.2010.12.015, 2011.

Maraseni, T. N. and Mitchell, C.: An assessment of carbon sequestration potential of riparian zone of Condamine Catchment, Queensland, Australia, Land Use Policy, 54, 139–146, https://doi.org/10.1016/j.landusepol.2016.02.013, 2016.

Mommer, L., Lenssen, J. P. M., Huber, H., Visser, E. J. W., and de Kroon, H.: Ecophysiological Determinants of Plant Performance under Flooding: A Comparative Study of Seven Plant Families, Journal of Ecology, 94, 1117–1129, 2006.

715 Morse, J. L., Ardón, M., and Bernhardt, E. S.: Greenhouse gas fluxes in southeastern U.S. coastal plain wetlands under contrasting land uses, Ecological Applications, 22, 264–280, https://doi.org/10.1890/11-0527.1, 2012.

Naiman, R. J. and Decamps, H.: The Ecology of Interfaces: Riparian Zones, Annual Review of Ecology and Systematics, 28, 621–658, 1997.

Pugh, T. A. M., Arneth, A., Kautz, M., Poulter, B., and Smith, B.: Important role of forest disturbances in the global biomass 720 turnover and carbon sinks, Nat Geosci, 12, 730–735, https://doi.org/10.1038/s41561-019-0427-2, 2019.

Raymond, P. A. and Saiers, J. E.: Event controlled DOC export from forested watersheds, Biogeochemistry, 100, 197–209, https://doi.org/10.1007/s10533-010-9416-7, 2010.

Ren, Y., Wang, D., and Li, X.: Impacts of Human Disturbances on Riparian Herbaceous Communities in a Chinese Karst River, Nature Environment and Pollution Technology, 18, 1107–1118, 2019.

725 Søvik, A. K. and Kløve, B.: Emission of N2O and CH4 from a constructed wetland in southeastern Norway, Science of The Total Environment, 380, 28–37, https://doi.org/10.1016/j.scitotenv.2006.10.007, 2007.

Steiger, J., Tabacchi, E., Dufour, S., Corenblit, D., and Peiry, J.-L.: Hydrogeomorphic processes affecting riparian habitat within alluvial channel-floodplain river systems: a review for the temperate zone, River Res. Applic., 21, 719–737, https://doi.org/10.1002/rra.879, 2005.

730 Still, C. J., Berry, J. A., Collatz, G. J., and DeFries, R. S.: Global distribution of C $_3$ and C $_4$ vegetation: Carbon cycle implications: C $_4$ PLANTS AND CARBON CYCLE, Global Biogeochem. Cycles, 17, 6-1-6–14, https://doi.org/10.1029/2001GB001807, 2003.

Sun, Q., Shi, K., Damerell, P., Whitham, C., Yu, G., and Zou, C.: Carbon dioxide and methane fluxes: Seasonal dynamics from inland riparian ecosystems, northeast China, Science of The Total Environment, 465, 48–55, 735 https://doi.org/10.1016/j.scitotenv.2013.01.036, 2013.

Sun, Q.-Q., Whitham, C., Shi, K., Yu, G.-H., and Sun, X.-W.: Nitrous oxide emissions from a waterbody in the Nenjiang basin, China, Hydrology Research, 43, 862–869, https://doi.org/10.2166/nh.2012.060, 2012.

Sutfin, N. A., Wohl, E. E., and Dwire, K. A.: Banking carbon: a review of organic carbon storage and physical factors influencing retention in floodplains and riparian ecosystems: BANKING CARBON, Earth Surf. Process. Landforms, 41, 38– 740 60, https://doi.org/10.1002/esp.3857, 2016.

Thorp, J. H., Thoms, M. C., and Delong, M. D.: The riverine ecosystem synthesis: biocomplexity in river networks across space and time, River Research and Applications, 22, 123–147, https://doi.org/10.1002/rra.901, 2006.

Vidon, P. G., Welsh, M. K., and Hassanzadeh, Y. T.: Twenty Years of Riparian Zone Research (1997–2017): Where to Next?, Journal of Environmental Quality, 48, 248–260, https://doi.org/10.2134/jeq2018.01.0009, 2019.

745 Wang, J., Wang, D., Ren, Y., and Wang, B.: Coupling relationships between soil microbes and soil nutrients under different hydrologic conditions in the riparian zone of the Lijiang River, Acta Ecol. Sin, 39, https://doi.org/10.5846/stxb201803260595, 2019a.

Wang, J., Wang, D., and Wang, B.: Soil Bacterial Diversity and its Determinants in the Riparian Zone of the Lijiang River, China, Current Science, 117, 1324, https://doi.org/10.18520/cs/v117/i8/1324-1332, 2019b.

750 Wang, J., Feng, L., Palmer, P. I., Liu, Y., Fang, S., Bösch, H., O'Dell, C. W., Tang, X., Yang, D., Liu, L., and Xia, C.: Large Chinese land carbon sink estimated from atmospheric carbon dioxide data, Nature, 586, 720–723, https://doi.org/10.1038/s41586-020-2849-9, 2020.

Wei, G.-W., Shu, Q., Luo, F.-L., Chen, Y.-H., Dong, B.-C., Mo, L.-C., Huang, W.-J., and Yu, F.-H.: Separating effects of clonal integration on plant growth during submergence and de-submergence, Flora, 246–247, 118–125,
755 https://doi.org/10.1016/j.flora.2018.08.004, 2018.

Wilson, J. S., Baldwin, D. S., Rees, G. N., and Wilson, B. P.: The effects of short-term inundation on carbon dynamics, microbial community structure and microbial activity in floodplain soil, River Research and Applications, 27, 213–225, https://doi.org/10.1002/rra.1352, 2011.

Zarnetske, J. P., Bouda, M., Abbott, B. W., Saiers, J., and Raymond, P. A.: Generality of Hydrologic Transport Limitation of
760 Watershed Organic Carbon Flux Across Ecoregions of the United States, Geophys. Res. Lett., 45, https://doi.org/10.1029/2018GL080005, 2018.

Zhang, T., Huang, X., Yang, Y., Li, Y., and Dahlgren, R. A.: Spatial and temporal variability in nitrous oxide and methane emissions in urban riparian zones of the Pearl River Delta, Environ Sci Pollut Res, 23, 1552–1564, https://doi.org/10.1007/s11356-015-5401-y, 2016.

765 Zhao, M., Han, G., Wu, H., Song, W., Chu, X., Li, J., Qu, W., Li, X., Wei, S., Eller, F., and Jiang, C.: Inundation depth affects ecosystem CO2 and CH4 exchange by changing plant productivity in a freshwater wetland in the Yellow River Estuary, Plant Soil, 454, 87–102, https://doi.org/10.1007/s11104-020-04612-2, 2020.

Zheng, X., Wang, M., Wang, Y., Shen, R., Li, J., J., H., M., K., Li, L., and Jin, J.: Comparison of manual and automatic methods for measurement of methane emission from rice paddy fields, Adv. Atmos. Sci., 15, 569–579,
770 https://doi.org/10.1007/s00376-998-0033-5, 1998.